Bayesian Neural Network Priors Revisited

Vincent Fortuin[*]   fortuin@inf.ethz.ch
ETH Zürich, Switzerland
Adrià Garriga-Alonso*   ag919@cam.ac.uk
University of Cambridge, United Kingdom
Florian Wenzel   wenzelfl@hu-berlin.de
Humboldt University of Berlin, Germany
Gunnar Rätsch   raetsch@inf.ethz.ch
ETH Zürich, Switzerland
Richard E. Turner   ret26@eng.cam.ac.uk
University of Cambridge, United Kingdom
Mark van der Wilk[†]   m.vdwilk@imperial.ac.uk
Imperial College London, United Kingdom
Laurence Aitchison[†]   laurence.aitchison@bristol.ac.uk
University of Bristol, United Kingdom

Abstract

Isotropic Gaussian priors are the *de facto* standard for modern Bayesian neural network inference. However, such simplistic priors are unlikely to either accurately reflect our true beliefs about the weight distributions, or to give optimal performance. We study summary statistics of (convolutional) neural network weights in networks trained using SGD. We find that in certain circumstances, these networks have heavy-tailed weight distributions, while convolutional neural network weights often display strong spatial correlations. Building these observations into the respective priors, we get improved performance on MNIST classification. Remarkably, we find that using a more accurate prior partially mitigates the cold posterior effect, by improving performance at high temperatures corresponding to exact Bayesian inference, while having less of an effect at small temperatures.

1. Introduction

In a Bayesian neural network (BNN), we put a prior $p(w)$ over the neural network parameters, and compute the posterior distribution over parameters conditioned on training data, $p(w|x, y) = p(y|w, x)p(w)/p(y|x)$. This procedure should give considerable advantages for reasoning about predictive uncertainty, which is especially relevant in the small data setting. Crucially, to perform Bayesian inference, we need to choose a prior that accurately reflects our beliefs about the parameters before seeing any data (Bayes, 1763; Gelman et al., 2013). However, the most common choice of the prior for BNN weights is the simplest one: the isotropic Gaussian. Isotropic Gaussians are used across almost all fields of Bayesian deep learning, ranging from variational inference (Dusenberry et al., 2020), to sampling-based

---

[*] Equal contribution.

[†] Equal contribution.

inference using SGLD (Zhang et al., 2019), and even to infinite networks (Lee et al., 2017; Garriga-Alonso et al., 2018). This is troubling, since isotropic Gaussian priors are almost certainly too simplistic. Indeed, artificially reducing posterior uncertainty using "cold" posteriors has been found to improve performance in Bayesian neural networks (BNNs) (Wenzel et al., 2020a). This is surprising, because if the prior and likelihood are accurately reflecting our beliefs, the Bayesian solution really should be optimal (Gelman et al., 2013). This raises the possibility that either the prior (Wenzel et al., 2020a) or likelihood (Aitchison, 2020), (or both) are ill-specified.

In this work, we study empirically whether isotropic Gaussian priors are indeed suboptimal for BNNs and whether this can explain the cold posterior effect. We analyse the performance of different BNN priors for different network architectures and compare them to the empirical weight distributions of maximum-likelihood solutions. We conclude that isotropic priors with heavier tails than the Gaussian are better suited for fully connected neural networks (FCNNs), while correlated Gaussian priors are better suited in the case of convolutional neural networks (CNNs). Thus, we would recommend the use of these priors instead of the widely-used isotropic Gaussians. While these priors can partially reduce the cold posterior effect in FCNNs, it remains more elusive in CNNs.

1.1. Contributions

Our main contributions are

- An analysis of the empirical weight distributions of SGD-trained neural networks with different architectures, suggesting that FCNNs learn heavy-tailed weight distributions (Sec. 3.1), while CNN weight distributions show significant correlations (Sec. 3.2).

- An empirical study of Bayesian FCCN performance, suggesting that heavy-tailed priors can outperform the widely-used Gaussian priors (Sec. 4.1).

- An empirical study of Bayesian CNN performance, suggesting that correlated Gaussian priors can outperform the isotropic ones (Sec. 4.2).

- An empirical study of the cold posterior effect in these models, suggesting that it can be reduced by choosing better priors in FCNNs, while the case is less clear in CNNs (Sec. 4).

1.2. Related Work

Previous work has investigated the performance implications of different neural network priors (Ghosh and Doshi-Velez, 2017; Wu et al., 2018; Atanov et al., 2018; Nalisnick, 2018; Overweg et al., 2019; Farquhar et al., 2019; Cui et al., 2020; Hafner et al., 2020; Ober and Aitchison, 2020). However, none of this work uses the empirical weight distributions of SGD-trained networks to inform BNN priors. For a more in-depth discussion see Appendix A.

2. Background: the Cold Posterior Effect

When performing inference in Bayesian models, we can temper the posterior by a positive temperature T, giving

$$\log p(w|x,y)^{\frac{1}{T}} = \frac{1}{T}[\log p(y|w,x) + \log p(w)] + Z(T) \tag{1}$$

for a normalizing constant $Z(T)$. Setting $T = 1$ gives the standard Bayesian posterior. The temperature parameter can be easily handled when simulating Langevin dynamics, used in molecular dynamics and MCMC (Leimkuhler and Matthews, 2012).

In their recent work, Wenzel et al. (2020a) have drawn attention to the effect that when the posterior is cooled down in BNNs (i.e., setting $T \ll 1$), the performance of the models often increases. Testing different hypotheses for potential problems with the inference, likelihood and prior, they conclude that the BNN priors (which were Gaussian in their experiments) are misspecified and could be one of the main causes of the "cold posterior effect". Reversing this argument, we can hypothesize that choosing better priors for BNNs should lead to a less pronounced cold posterior effect, which we can use to evaluate different candidate priors.

3. Empirical analysis of neural network weights

We trained fully connected neural networks (FCNNs) and convolutional neural networks (CNNs) with SGD on the task of MNIST handwritten digit recognition (LeCun et al., 1998) and analysed the empirical weight distributions. Intuitively, the more a BNN prior deviates from the empirical weight distribution reached by this training, the less probability mass the posterior will assign to the maximum-likelihood (ML) solution. This can be easily seen, since the posterior probability for the ML solution is $p(w_{ML}|x,y) \propto p(y|w_{ML},x)\,p(w_{ML})$, which scales linearly with the prior probability $p(w_{ML})$. Since BNNs are generally rather believed to be underfitting (Neal, 1995; Wenzel et al., 2020a; Dusenberry et al., 2020), we hypothesize that a prior should work better if it allows the posterior to assign more probability mass to the ML solution.

To explicitly contrast the empirical weights with the Gaussian distributional assumption of many prior works, we compare the distributions to the same number of weights sampled from a Gaussian with the same mean and variance as the empirical distribution. For this Gaussian weight sample, as well as the empirical ones, we can then compute the marginal distribution over weight values and the weight correlations across rows and columns (or respectively in CNNs, filters and channels). To increase the statistical power, we can average these distributions over several SGD runs.

Note that for ease of exposition, the figures in this section are just showing the results for a single layer out of each network. However, the observations readily extend to the other layers as well (see Appendix B).

3.1. Are neural network weights heavy tailed?

We can see in Figure 1 that the weight values of the FCNNs and CNNs follow a more heavy-tailed distribution than a Gaussian. Judging from the Q-Q plots, they seem to be
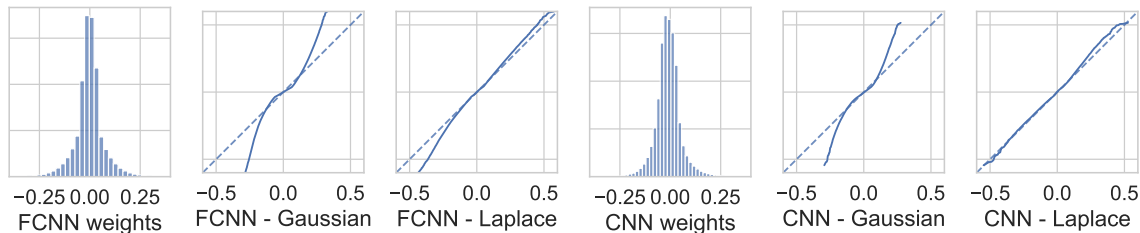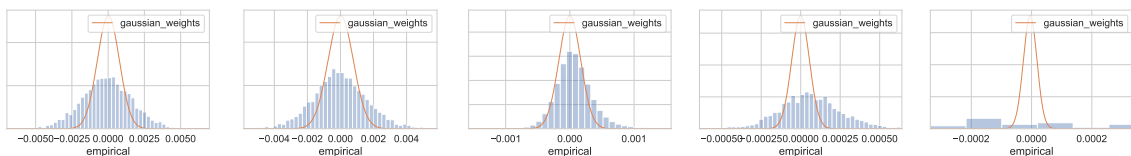
Figure 1: Empirical marginal weight distributions of FCNNs and CNNs trained with SGD on MNIST. We show marginal weight histograms and Q-Q plots with different distributions. It can be seen that heavy-tailed distributions (e.g., Laplace) yield a better fit than Gaussians for the empirical weight marginals.

(a) FCNN, cols   (b) FCNN, rows   (c) CNN, cols   (d) CNN, rows   (e) CNN, spatial

Figure 2: Distributions of off-diagonal elements in the empirical covariances of the weights of FCNNs and CNNs trained with SGD on MNIST. The empirical distributions are plotted as histograms, while the idealized random Gaussian weights are overlaid in orange. We see that the covariances of the empirical weights are more heavy-tailed than for the Gaussian weights.

better approximated by a Laplace distribution. This suggests that BNN priors for these models might benefit from being more heavy-tailed than isotropic Gaussians.

3.2. Are neural network weights correlated?

In contrast to the isotropic Gaussian, the empirical weight distributions of FCNNs show some significant correlations among rows and columns of the weight matrices (Fig. B.1). This can be seen especially well by comparing the distribution of off-diagonal elements of the empirical covariance matrices (Fig. 2). We see that the empirical weights (blue histograms) have a more heavy-tailed distribution of off-diagonal elements than the randomly sampled Gaussian weights (orange kernel density estimate).

Interestingly, this is also true for CNN weights (Fig. B.2). The off-diagonal elements of their empirical covariance matrices are also more heavy-tailed than for isotropic Gaussian weights (Fig. 2). Crucially, most of these correlations seem to occur spatially, that is, between weights within the same CNN filter (Fig. 3). This could potentially be due to the smoothness and translation equivariance properties of natural images (Simoncelli, 2009).

These findings suggest that better priors could be designed by explicitly taking this correlation structure into account. We hypothesize that multivariate distributions with non-diagonal covariance matrices could be good candidates for CNN priors, especially when the covariances are large for neighboring pixels within the CNN filters (see Sec. 4.2).
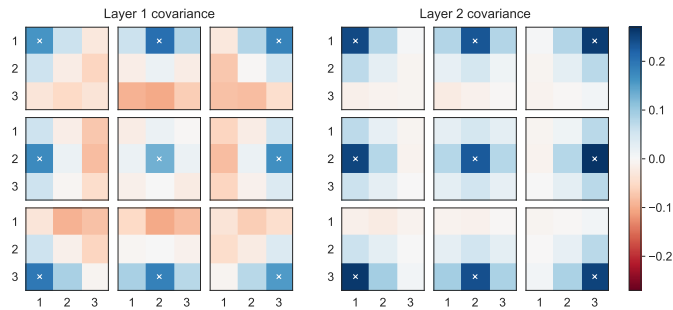
Figure 3: Spatial covariance of the weights within CNN filters, multiplied by the number of input channels (1 for Layer 1, 64 for Layer 2). The weights correlate strongly with neighboring pixels, and anti-correlate (Layer 1) or do not correlate (Layer 2) with distant ones. Each delineated square shows the covariances of a filter location (marked with ×) with all other locations.

4. Empirical study of Bayesian neural network priors

We again performed experiments on the MNIST handwritten digit data set (LeCun et al., 1998). We compare Bayesian FCNNs and Bayesian CNNs on this task. For the BNN inference, we use Stochastic Gradient Markov Chain Monte Carlo (SG-MCMC), following Wenzel et al. (2020a) and Zhang et al. (2019). Additional experimental results can be found in Appendix B, inference diagnostics in Appendix C, and implementation details in Appendix F.

4.1. Bayesian FCNN performance with different priors

Following our observations from the empirical weight distributions (Sec. 3.1), we hypothesized that heavy-tailed priors should work better than Gaussian ones for Bayesian FCNNs. We tested this by performing BNN inference with the same network architecture as above using different priors (for details about the priors, see Appendix D). We report the predictive error and log likelihood on the MNIST test set. We follow Ovadia et al. (2019) in reporting the calibration of the uncertainty estimates on rotated MNIST digits and the out-of-distribution (OOD) detection accuracy on FashionMNIST (Xiao et al., 2017). For more details about our evaluation metrics, we refer to Appendix E.

We observe that the heavy-tailed priors do indeed outperform the Gaussian one for all metrics except for the calibration error (Fig. 4). This suggests that Gaussian priors over the weights of feedforward networks induce poor priors in the function space and inhibit the posterior from assigning probability mass to high-likelihood solutions, such as the SGD solutions analysed above (Sec. 3). Moreover, we find that the cold posterior effect is less pronounced when using heavy-tailed priors.

4.2. Bayesian CNN performance with different priors

We repeated the same experiment for Bayesian CNNs. Following our observations from the empirical weights (Sec. 3.1), in this case we might also expect the heavy-tailed priors to outperform the Gaussian one. The results in terms of performance alone are less striking

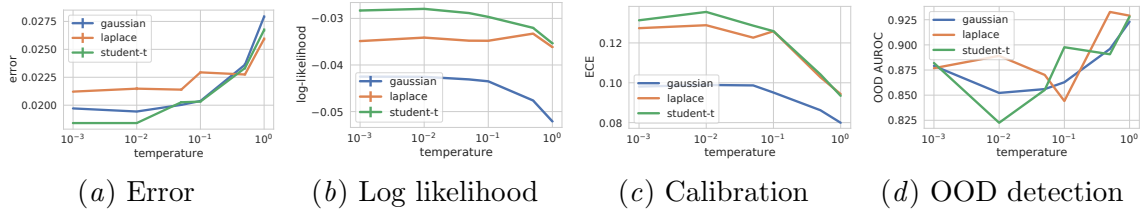(a) Error   (b) Log likelihood   (c) Calibration   (d) OOD detection

Figure 4: Cold posterior effect of Bayesian FCNNs with different priors on MNIST in terms of different metrics. We see that the heavy-tailed priors generally lead to a less pronounced cold posterior effect than the Gaussian ones.
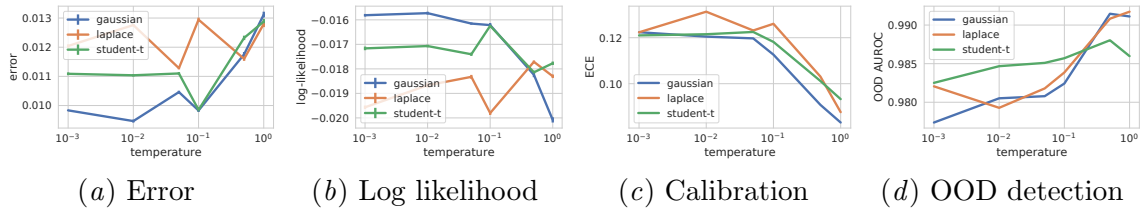

(a) Error   (b) Log likelihood   (c) Calibration   (d) OOD detection

Figure 5: Cold posterior effect of Bayesian CNNs with different priors on MNIST in terms of different metrics. We see that the heavy-tailed priors generally lead to a less pronounced cold posterior effect than the Gaussian ones.

(a) Error   (b) Log likelihood   (c) Calibration   (d) OOD detection
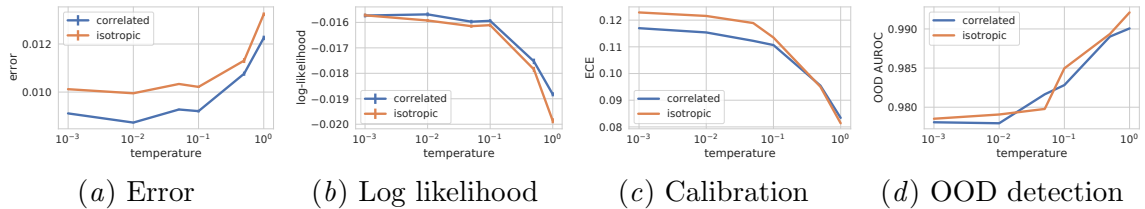
Figure 6: Cold posterior effect of Bayesian CNNs with different priors on MNIST in terms of different metrics. We see that the correlated prior has a better performance but roughly the same cold posterior effect as the isotropic one.

here than in the FCNN experiments, and when cooling down the posterior, the Gaussian prior often outperforms the heavy-tailed ones (Fig. 5). However, in the true posterior ($T = 1$), we see that the heavy-tailed priors generally perform slightly better than the Gaussian, even though this effect might not be significant. Moreover, we again observe that the cold posterior effect is less pronounced with heavy-tailed priors.

Apart from the marginal weight priors, following our correlation analysis (Sec. 3.2) we would expect to improve the prior when introducing weight correlations. We did this by defining a multivariate Gaussian prior with nonzero covariance between weights within each CNN filter, where the covariance is defined by a radial basis function (RBF) kernel, such that it decays smoothly with increasing distance in pixel space. We describe this prior in more detail in Appendix D. For this correlated prior, we observe that it does indeed improve the performance compared to the isotropic Gaussian one (Fig. 6). However, the cold posterior effect is not reduced as significantly as in the previous experiments and thus remains more elusive for CNNs.

5. Conclusion

We have shown that especially in fully-connected BNNs, heavy-tailed non-Gaussian priors can yield a better performance across many metrics and also fit the empirical weight distributions of maximum-likelihood solutions better. Moreover, they seem to partially alleviate the cold posterior effect.

In contrast, in convolutional BNNs, the performance benefit of heavy-tailed priors seems less obvious, although they also fit the empirical weights better and alleviate the cold posterior effect. Moreover, CNNs seem to exhibit significant correlations in the empirical weight distributions, especially between weights within a filter. Including such correlations into the prior improves the performance, but does not seem to alleviate the cold posterior effect.

References

Laurence Aitchison. A statistical theory of cold posteriors in deep neural networks. *arXiv preprint arXiv:2008.05912*, 2020.

Andrei Atanov, Arsenii Ashukha, Kirill Struminsky, Dmitry Vetrov, and Max Welling. The deep weight prior. *arXiv preprint arXiv:1810.06943*, 2018.

Thomas Bayes. Lii. an essay towards solving a problem in the doctrine of chances. by the late rev. mr. bayes, frs communicated by mr. price, in a letter to john canton, amfr s. *Philosophical transactions of the Royal Society of London*, (53):370–418, 1763.

I Bellido and Emile Fiesler. Do backpropagation trained neural networks have normal weight distributions? In *International Conference on Artificial Neural Networks*, pages 772–775. Springer, 1993.

Patrick Billingsley. The Lindeberg-Lévy theorem for martingales. *Proceedings of the American Mathematical Society*, 12(5):788–792, 1961.

Christopher M Bishop. *Pattern recognition and machine learning.* Springer, 2006.

Tianyu Cui, A. Havulinna, P. Marttinen, and S. Kaski. Informative gaussian scale mixture priors for bayesian neural networks. *arXiv preprint arXiv:2002.10243*, 2020.

Michael W Dusenberry, Ghassen Jerfel, Yeming Wen, Yi-an Ma, Jasper Snoek, Katherine Heller, Balaji Lakshminarayanan, and Dustin Tran. Efficient and scalable bayesian neural nets with rank-1 factors. *arXiv preprint arXiv:2005.07186*, 2020.

Sebastian Farquhar, Michael Osborne, and Yarin Gal. Radial bayesian neural networks: Robust variational inference in big models. *arXiv preprint arXiv:1907.00865*, 2019.

David J Field. Relations between the statistics of natural images and the response properties of cortical cells. *Josa a*, 4(12):2379–2394, 1987.

Adrià Garriga-Alonso, Carl Edward Rasmussen, and Laurence Aitchison. Deep convolutional networks as shallow gaussian processes. *arXiv preprint arXiv:1808.05587*, 2018.

Carl Friedrich Gauss. *Theoria motvs corporvm coelestivm in sectionibvs conicis solem ambientivm.* Sumtibus F. Perthes et IH Besser, 1809.

Andrew Gelman, John B Carlin, Hal S Stern, David B Dunson, Aki Vehtari, and Donald B Rubin. *Bayesian data analysis.* CRC press, 2013.

Soumya Ghosh and Finale Doshi-Velez. Model selection in bayesian neural networks via horseshoe priors. *arXiv preprint arXiv:1705.10388*, 2017.

Tilmann Gneiting and Adrian E Raftery. Strictly proper scoring rules, prediction, and estimation. *Journal of the American statistical Association*, 102(477):359–378, 2007.

Jinwook Go and Chulhee Lee. Analyzing weight distribution of neural networks. In *IJCNN'99. International Joint Conference on Neural Networks. Proceedings (Cat. No. 99CH36339)*, volume 2, pages 1154–1157. IEEE, 1999.

Danijar Hafner, Dustin Tran, Timothy Lillicrap, Alex Irpan, and James Davidson. Noise contrastive priors for functional uncertainty. In *Uncertainty in Artificial Intelligence*, pages 905–914. PMLR, 2020.

Friedrich Robert Helmert. Über die berechnung des wahrscheinlichen fehlers aus einer endlichen anzahl wahrer beobachtungsfehler. *Z. Math. U. Physik*, 20(1875):300–303, 1875.

Theofanis Karaletsos and Thang D Bui. Hierarchical gaussian process priors for bayesian neural network weights. *arXiv preprint arXiv:2002.04033*, 2020.

Alex Kendall and Yarin Gal. What uncertainties do we need in bayesian deep learning for computer vision? In *Advances in neural information processing systems*, pages 5574–5584, 2017.

Pierre Simon Laplace. Mémoire sur la probabilité de causes par les évenements. *Memoire de l'Academie Royale des Sciences*, 1774.

Yann LeCun, Léon Bottou, Yoshua Bengio, and Patrick Haffner. Gradient-based learning applied to document recognition. *Proceedings of the IEEE*, 86(11):2278–2324, 1998.

Jaehoon Lee, Yasaman Bahri, Roman Novak, Samuel S Schoenholz, Jeffrey Pennington, and Jascha Sohl-Dickstein. Deep neural networks as gaussian processes. *arXiv preprint arXiv:1711.00165*, 2017.

Benedict Leimkuhler and Charles Matthews. Rational Construction of Stochastic Numerical Methods for Molecular Sampling. *Applied Mathematics Research eXpress*, 2013(1):34–56, 06 2012. ISSN 1687-1200. doi: 10.1093/amrx/abs010.

Christos Louizos and Max Welling. Multiplicative normalizing flows for variational bayesian neural networks. *arXiv preprint arXiv:1703.01961*, 2017.

J Lüroth. Vergleichung von zwei werthen des wahrscheinlichen fehlers. *Astronomische Nachrichten*, 87:209, 1876.

Siwei Lyu and Eero P Simoncelli. Modeling multiscale subbands of photographic images with fields of gaussian scale mixtures. *IEEE Transactions on pattern analysis and machine intelligence*, 31(4):693–706, 2008.

Chao Ma, Yingzhen Li, and José Miguel Hernández-Lobato. Variational implicit processes. In *International Conference on Machine Learning*, pages 4222–4233, 2019.

David JC MacKay. A practical bayesian framework for backpropagation networks. *Neural computation*, 4(3):448–472, 1992.

Wesley J Maddox, Pavel Izmailov, Timur Garipov, Dmitry P Vetrov, and Andrew Gordon Wilson. A simple baseline for bayesian uncertainty in deep learning. In *Advances in Neural Information Processing Systems*, pages 13153–13164, 2019.

Alexander G de G Matthews, Mark Rowland, Jiri Hron, Richard E Turner, and Zoubin Ghahramani. Gaussian process behaviour in wide deep neural networks. *arXiv preprint arXiv:1804.11271*, 2018.

Mahdi Pakdaman Naeini, Gregory F Cooper, and Milos Hauskrecht. Obtaining well calibrated probabilities using bayesian binning. In *Proceedings of the... AAAI Conference on Artificial Intelligence. AAAI Conference on Artificial Intelligence*, volume 2015, page 2901. NIH Public Access, 2015.

Eric Nalisnick, José Miguel Hernández-Lobato, and Padhraic Smyth. Dropout as a structured shrinkage prior. In *International Conference on Machine Learning*, pages 4712–4722. PMLR, 2019.

Eric Thomas Nalisnick. *On priors for bayesian neural networks*. PhD thesis, UC Irvine, 2018.

Radford M Neal. Bayesian training of backpropagation networks by the hybrid monte carlo method. Technical report, Citeseer, 1992.

Radford M Neal. Bayesian leaning for neural networks, 1995.

Sebastian W Ober and Laurence Aitchison. Global inducing point variational posteriors for bayesian neural networks and deep gaussian processes. *arXiv preprint arXiv:2005.08140*, 2020.

Bruno A Olshausen and David J Field. Sparse coding with an overcomplete basis set: A strategy employed by v1? *Vision research*, 37(23):3311–3325, 1997.

Kazuki Osawa, Siddharth Swaroop, Mohammad Emtiyaz E Khan, Anirudh Jain, Runa Eschenhagen, Richard E Turner, and Rio Yokota. Practical deep learning with bayesian principles. In *Advances in neural information processing systems*, pages 4287–4299, 2019.

Yaniv Ovadia, Emily Fertig, Jie Ren, Zachary Nado, David Sculley, Sebastian Nowozin, Joshua Dillon, Balaji Lakshminarayanan, and Jasper Snoek. Can you trust your model's uncertainty? evaluating predictive uncertainty under dataset shift. In *Advances in Neural Information Processing Systems*, pages 13991–14002, 2019.

Hiske Overweg, Anna-Lena Popkes, Ari Ercole, Yingzhen Li, José Miguel Hernández-Lobato, Yordan Zaykov, and Cheng Zhang. Interpretable outcome prediction with sparse bayesian neural networks in intensive care. *arXiv preprint arXiv:1905.02599*, 2019.

Tim Pearce, Russell Tsuchida, Mohamed Zaki, Alexandra Brintrup, and Andy Neely. Expressive priors in bayesian neural networks: Kernel combinations and periodic functions. In *Uncertainty in Artificial Intelligence*, pages 134–144. PMLR, 2020.

Stefano Peluchetti, Stefano Favaro, and Sandra Fortini. Stable behaviour of infinitely wide deep neural networks. In *International Conference on Artificial Intelligence and Statistics*, pages 1137–1146. PMLR, 2020.

Eero P Simoncelli. Capturing visual image properties with probabilistic models. In *The Essential Guide to Image Processing*, pages 205–223. Elsevier, 2009.

Anuj Srivastava, Ann B Lee, Eero P Simoncelli, and S-C Zhu. On advances in statistical modeling of natural images. *Journal of mathematical imaging and vision*, 18(1):17–33, 2003.

Student. The probable error of a mean. *Biometrika*, pages 1–25, 1908.

Shengyang Sun, Guodong Zhang, Jiaxin Shi, and Roger Grosse. Functional variational bayesian neural networks. *arXiv preprint arXiv:1903.05779*, 2019.

Jakub Swiatkowski, Kevin Roth, Bastiaan S Veeling, Linh Tran, Joshua V Dillon, Stephan Mandt, Jasper Snoek, Tim Salimans, Rodolphe Jenatton, and Sebastian Nowozin. The k-tied normal distribution: A compact parameterization of gaussian mean field posteriors in bayesian neural networks. *arXiv preprint arXiv:2002.02655*, 2020.

Robert Tibshirani. Regression shrinkage and selection via the lasso. *Journal of the Royal Statistical Society: Series B (Methodological)*, 58(1):267–288, 1996.

Russell Tsuchida, Fred Roosta, and Marcus Gallagher. Richer priors for infinitely wide multi-layer perceptrons. *arXiv preprint arXiv:1911.12927*, 2019.

Mariia Vladimirova, Jakob Verbeek, Pablo Mesejo, and Julyan Arbel. Understanding priors in bayesian neural networks at the unit level. In *International Conference on Machine Learning*, pages 6458–6467. PMLR, 2019.

Martin J Wainwright and Eero Simoncelli. Scale mixtures of gaussians and the statistics of natural images. *Advances in neural information processing systems*, 12:855–861, 1999.

Florian Wenzel, Kevin Roth, Bastiaan S Veeling, Jakub Świ atkowski, Linh Tran, Stephan Mandt, Jasper Snoek, Tim Salimans, Rodolphe Jenatton, and Sebastian Nowozin. How good is the bayes posterior in deep neural networks really? In *International Conference on Machine Learning*, 2020a.

Florian Wenzel, Jasper Snoek, Dustin Tran, and Rodolphe Jenatton. Hyperparameter ensembles for robustness and uncertainty quantification. In *Advances in Neural Information Processing Systems*, 2020b.

Andrew Gordon Wilson and Pavel Izmailov. Bayesian deep learning and a probabilistic perspective of generalization. *arXiv preprint arXiv:2002.08791*, 2020.

Anqi Wu, Sebastian Nowozin, Edward Meeds, Richard E Turner, José Miguel Hernández-Lobato, and Alexander L Gaunt. Deterministic variational inference for robust bayesian neural networks. *arXiv preprint arXiv:1810.03958*, 2018.

Han Xiao, Kashif Rasul, and Roland Vollgraf. Fashion-mnist: a novel image dataset for benchmarking machine learning algorithms. *arXiv preprint arXiv:1708.07747*, 2017.

Greg Yang. Wide feedforward or recurrent neural networks of any architecture are gaussian processes. In *Advances in Neural Information Processing Systems*, pages 9951–9960, 2019.

Ruqi Zhang, Chunyuan Li, Jianyi Zhang, Changyou Chen, and Andrew Gordon Wilson. Cyclical stochastic gradient mcmc for bayesian deep learning. *arXiv preprint arXiv:1902.03932*, 2019.

Appendix A. Detailed Related Work

Empirical analysis of weight distributions. There is some history in neuroscience of analysing the statistics of data to inform inductive priors for learning algorithms, especially when it comes to vision (Simoncelli, 2009). For instance, it has been noted that correlations help in modeling natural images (Srivastava et al., 2003), as well as sparsity in the parameters (Field, 1987; Olshausen and Field, 1997), and the use of Gaussian scale mixtures (Wainwright and Simoncelli, 1999; Lyu and Simoncelli, 2008). In the context of machine learning, the empirical weight distributions of standard neural networks have also been studied before (Bellido and Fiesler, 1993; Go and Lee, 1999), but these works have not systematically compared different architectures and did not use their insights to inform Bayesian prior choices.

BNNs in practice. Since the inception of Bayesian neural networks, scholars have thought about choosing good priors for them, including hierarchical (MacKay, 1992) and heavy-tailed ones (Neal, 1995). In the context of infinite-width limits of such networks (Lee et al., 2017; Matthews et al., 2018; Garriga-Alonso et al., 2018; Yang, 2019; Tsuchida et al., 2019) it has also been shown that heavy-tailed priors can lead to more interesting properties than finite-variance ones (Neal, 1995; Peluchetti et al., 2020). Moreover, it has been shown that the activations in deep neural networks grow more heavy-tailed with increasing depth (Vladimirova et al., 2019) and that the popular dropout regularization is related to sparsity-inducing priors (Nalisnick et al., 2019). Nonetheless, most state-of-the-art BNN methods still use simple isotropic Gaussian priors (Osawa et al., 2019; Zhang et al., 2019; Maddox et al., 2019; Wilson and Izmailov, 2020; Dusenberry et al., 2020). It has been hypothesized that this could be one of the reasons why BNNs are still not convincingly outperforming standard neural networks on many tasks (Wenzel et al., 2020a).

Alternative BNN priors. While many interesting distributions have been proposed as variational posteriors for BNNs (Louizos and Welling, 2017; Farquhar et al., 2019; Swiatkowski et al., 2020; Dusenberry et al., 2020), these approaches have still relied on simple Gaussian priors. Although a few different priors have been proposed for BNNs, these were mostly designed for specific tasks (Atanov et al., 2018; Ghosh and Doshi-Velez, 2017; Overweg et al., 2019; Nalisnick, 2018; Cui et al., 2020; Hafner et al., 2020) or relied heavily on non-standard inference methods (Sun et al., 2019; Ma et al., 2019; Karaletsos and Bui, 2020; Pearce et al., 2020).

Our work. In this work we explicitly study the question of whether non-Gaussian priors are generally useful (or even necessary) for Bayesian neural networks. We make an attempt to answer this question for different neural network architectures and also compare the priors to the empirical distributions of weights in networks trained via maximum likelihood. Moreover, we used reliable Markov Chain Monte Carlo (MCMC) BNN inference (Neal, 1992; Zhang et al., 2019; Wenzel et al., 2020a) in our experiments to be able to make claims about the true posteriors of the models. This is in contrast to many of the works mentioned above, which used variational inference approaches for sake or their computational benefits.

Appendix B. Additional experimental results

B.1. Covariance matrices

Here we report the full covariance matrices for the layers that were analysed above (Sec. 3.2). The covariances of the FCNN weights are shown in Figure B.1 and of the CNN weights in Figure B.2.
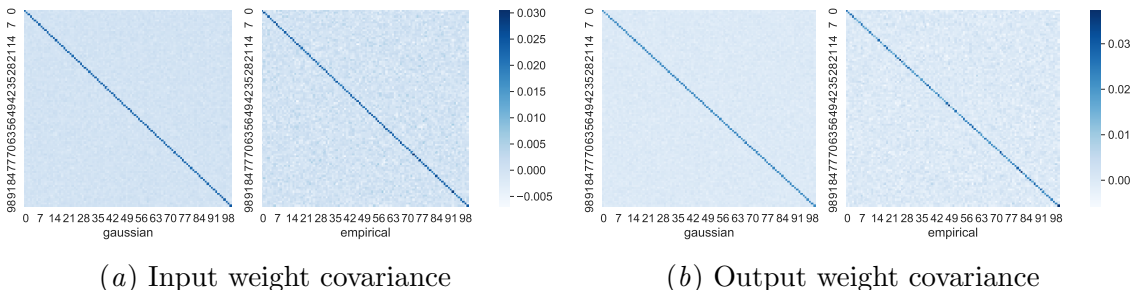

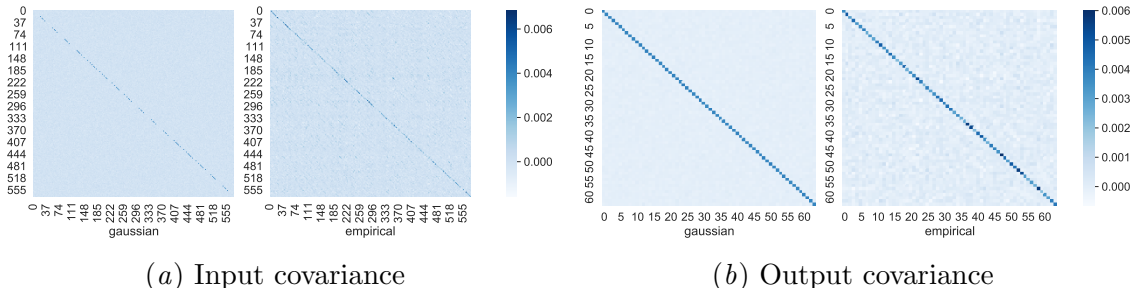(*a*) Input weight covariance   (*b*) Output weight covariance

Figure B.1: Empirical covariances of the weights of FCNNs trained with SGD on MNIST. We see that they contain more systematic correlations than the isotropic Gaussian.

(*a*) Input covariance   (*b*) Output covariance

Figure B.2: Empirical covariances of the weights of CNNs trained with SGD on MNIST. We see that they also contain more systematic correlations than the isotropic Gaussian.

B.2. Empirical weight results for the other layers

In Section 3 we exemplarily report results for the respective second layers of our FCNN and CNN. Here, we report the same results for the other layers for sake of completeness. The FCNN results are shown in Figures B.3, B.4, B.5, and B.6 and the CNN results in Figures B.7 and B.8.

B.3. BNN performances of untempered posteriors

Here we report the BNN performances from the experiments in Section 4 for the true Bayesian posteriors ($T = 1$) for ease of comparison. The FCNN performances with heavy-tailed and Gaussian priors are shown in Figure B.9, the CNN performances with heavy-tailed and Gaussian priors in Figure B.10, and the CNN performances with isotropic and correlated Gaussian priors in Figure B.11.

(*a*) Layer 1, columns   (*b*) Layer 1, rows   (*c*) Layer 3, columns   (*d*) Layer 3, rows
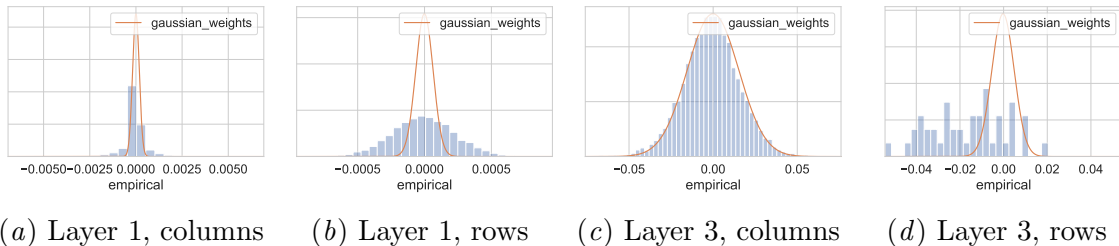
Figure B.3: Distributions of off-diagonal elements in the empirical covariances of the weights of the FCNN in the other layers. The empirical distributions are plotted as histograms, while the idealized random Gaussian weights are overlaid in orange. We see that the covariances of the empirical weights are more heavy-tailed than for the Gaussian weights.
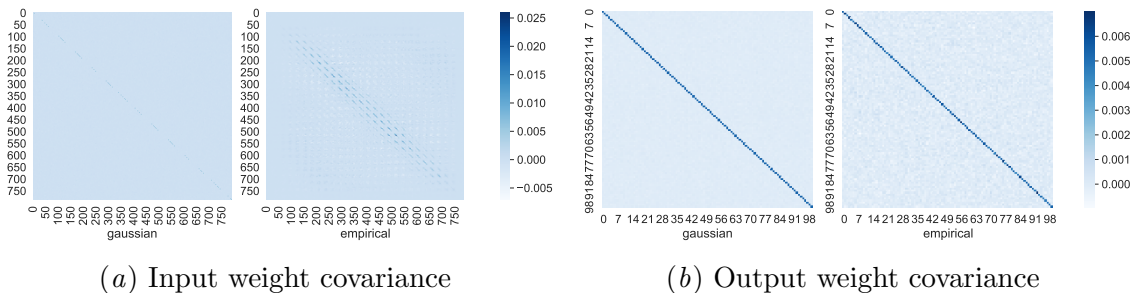

(*a*) Input weight covariance   (*b*) Output weight covariance

Figure B.4: Empirical covariances of the weights of the FCNN in the first layer. We see that they contain more systematic correlations than the isotropic Gaussian.

Appendix C. Inference diagnostics

In order to check the correctness of our SG-MCMC inference, we estimated the temperature of the sampler using the two different methods from Wenzel et al. (2020a), namely the *kinetic temperature* and the *configurational temperature*.

The kinetic temperature is derived from the sampler's momentum $\boldsymbol{m} \in \mathbb{R}^d$. The inner product $\frac{1}{d}\boldsymbol{m}^\mathsf{T}\boldsymbol{M}^{-1}\boldsymbol{m}$, for the (in this case diagonal) mass matrix $\boldsymbol{M}$, is an estimate of the scaled variance of the momenta, and should, in expectation, be equal to the desired temperature. In contrast, the configurational temperature is $\frac{1}{d}\boldsymbol{\theta}^\mathsf{T}\nabla H(\boldsymbol{\theta}, \boldsymbol{m})$. In expectation, this should also equal T. Using subsets of a parameter or momentum also yields estimators of the temperature.

In both cases, we estimate the mean and its standard error from a weighted average of parameters or momenta. That is, for each separate NN weight matrix or bias vector, we estimate its kinetic and configurational temperature using the expressions above. Then, we take their average, weighted by how many elements each matrix or vector has, and approximate its weighted standard error[1].

We show the estimated temperatures in Figures C.1, C.2, and C.3, as a mean ± two standard errors. The desired temperature is shown as a dotted horizontal line. The kinetic temperatures generally agree well with the true temperatures, so our sampler works as

---

1. Following the code from https://stats.stackexchange.com/q/33959

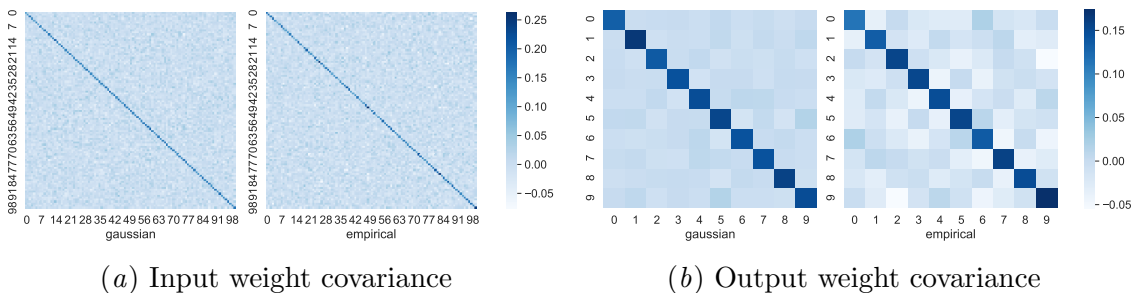(a) Input weight covariance (b) Output weight covariance

Figure B.5: Empirical covariances of the weights of the FCNN in the third layer. We see that they contain more systematic correlations than the isotropic Gaussian.
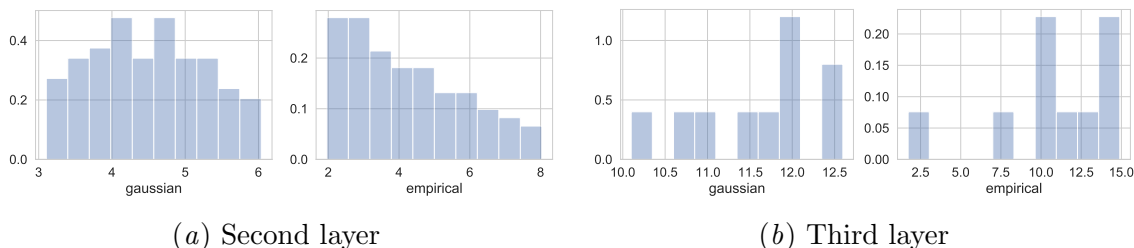

(a) Second layer (b) Third layer

Figure B.6: Distributions of singular values of the weight matrices of the FCNN in the other layers. We see that the spectra of the empirical weights decay faster than the ones of the Gaussian weights.

expected there. The configurational temperature estimates have a higher variance than the kinetic ones. Their error bars mostly include the true temperatures, but their means are usually too low. Thus, the sampler is still within the tolerance levels of working correctly there, but there could be some small inaccuracies.

Appendix D. Priors for Bayesian Neural Networks

In this study, we contrast the widely used Gaussian priors with more heavy-tailed priors, especially Laplace and Student-t distributions. We chose these distributions mostly based on our observations regarding the empirical weight distributions of trained networks (see Fig. 1 and Sec. 3) and for their ease of implementation and optimization. We now give a quick overview over these different distributions and their most salient properties.

Gaussian The Gaussian distribution (Gauss, 1809) is the *de-facto* standard for BNN priors in recent work (Wenzel et al., 2020a; Wilson and Izmailov, 2020; Zhang et al., 2019). Its probability density function (PDF) is

$$p(x; \mu, \sigma^2) = \frac{1}{\sqrt{2\pi\sigma^2}} \exp\left(-\frac{(x-\mu)^2}{2\sigma^2}\right)$$

It is attractive, because it is the central limit of all finite-variance distributions (Billingsley, 1961) and the maximum entropy distribution for a given mean and scale (Bishop, 2006).

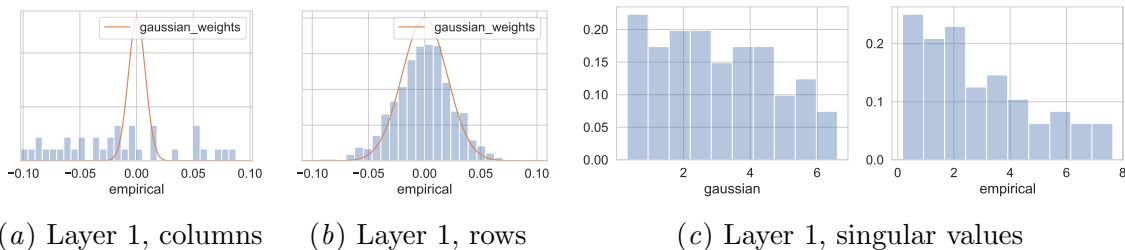(a) Layer 1, columns   (b) Layer 1, rows   (c) Layer 1, singular values

Figure B.7: Distributions of off-diagonal elements in the empirical covariances of the weights and singular values of the CNN in the other layer. The empirical distributions are plotted as histograms, while the idealized random Gaussian weights are overlaid in orange. We see that the covariances of the empirical weights are more heavy-tailed than for the Gaussian weights and that the singular value spectrum for the empirical weights decays faster than the Gaussian ones.

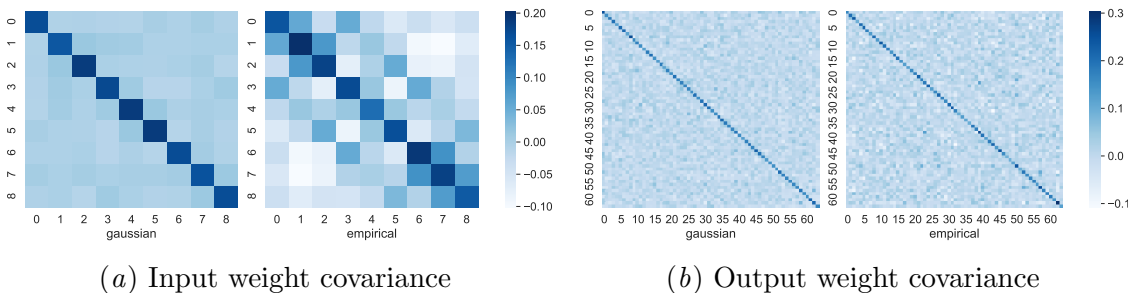(a) Input weight covariance   (b) Output weight covariance

Figure B.8: Empirical covariances of the weights of the CNN in the first layer. We see that they contain more systematic correlations than the isotropic Gaussian.

However, its tails are relatively light compared to some of the other distributions that we will consider.

Laplace The Laplace distribution (Laplace, 1774) has heavier tails than the Gaussian and is discontinuous at $x = \mu$. Its PDF is

$$p(x; \mu, b) = \frac{1}{2b} \exp\left(-\frac{|x - \mu|}{b}\right)$$

It is often used in the context of lasso regression, where it encourages sparsity in the learned weights (Tibshirani, 1996).

Student-t The Student-t distribution characterizes the mean of a finite number of samples from a Gaussian distribution with respect to the true mean (Student, 1908). Its PDF is

$$p(x; \mu, \nu) = \frac{\Gamma(\frac{\nu+1}{2})}{\Gamma(\frac{\nu}{2})\sqrt{\nu\pi}} \left(1 + \frac{(x - \mu)^2}{\nu}\right)^{-\frac{\nu+1}{2}},$$

where Γ is the gamma function and ν are the degrees of freedom. The Student-t also arises as the marginal distribution over Gaussians with an inverse-Gamma prior over the

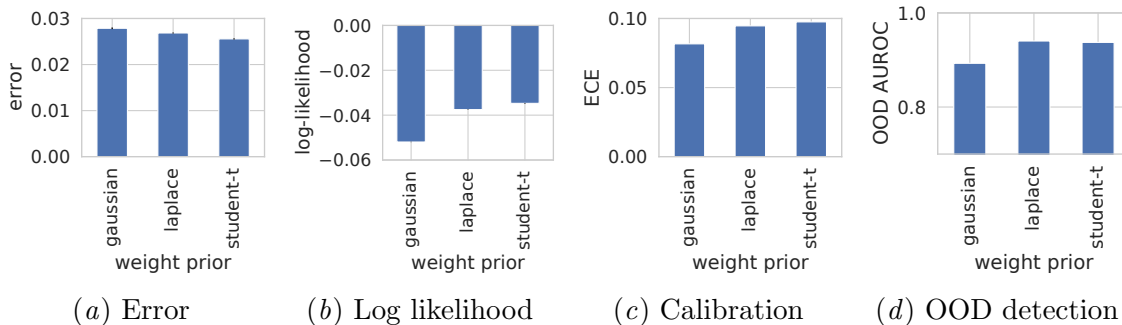(a) Error (b) Log likelihood (c) Calibration (d) OOD detection

Figure B.9: Performance of Bayesian FCNNs with different priors on MNIST in terms of different metrics. We see that the heavy-tailed priors perform better than the Gaussian ones, except in terms of expected calibration.
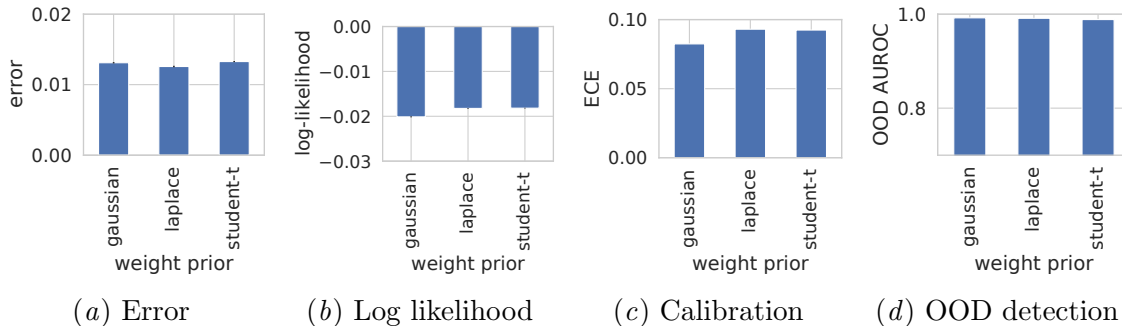

(a) Error (b) Log likelihood (c) Calibration (d) OOD detection

Figure B.10: Performance of Bayesian CNNs with different priors on MNIST in terms of different metrics. We see that the Gaussian prior performs as well as the other ones.

variances (Helmert, 1875; Lüroth, 1876). For $\nu \to \infty$, the Student-t distribution approaches the Gaussian. For any finite ν it has heavier tails than the Gaussian. Its k'th moment is only finite for $\nu > k$. The ν parameter thus offers a convenient way to adjust the heaviness of the tails. Unless otherwise stated, we set $\nu = 3$ in our experiments, such that the distribution has rather heavy tails, while still having a finite mean and variance.

Multivariate Gaussian with RBF covariance For our correlated Bayesian CNN priors, we use multivariate Gaussian priors

$$p(\boldsymbol{x}; \boldsymbol{\mu}, \boldsymbol{\Sigma}) = \frac{1}{\sqrt{(2\pi)^d \det \boldsymbol{\Sigma}}} \exp\left(-\frac{1}{2}(\boldsymbol{x} - \boldsymbol{\mu})^\top \boldsymbol{\Sigma}^{-1}(\boldsymbol{x} - \boldsymbol{\mu})\right) \;,$$

where d is the dimensionality.

In our experiments, we set $\boldsymbol{\mu} = \mathbf{0}$ and define the covariance $\boldsymbol{\Sigma}$ to be block-diagonal, such that the covariance between weights in different filters is 0 and between weights in the same filter is given by an RBF kernel on the pixel distances. Formally, for the weights $w_{i,j}$ and $w_{i',j'}$ in filters i and i' and for pixels j and j', the covariance is

$$\text{cov}(w_{i,j}, w_{i',j'}) = \begin{cases} \sigma^2 \exp\left(\frac{-d(j,j')}{\lambda}\right) & \text{if } i = i' \\ 0 & \text{else} \end{cases} \;,$$

17

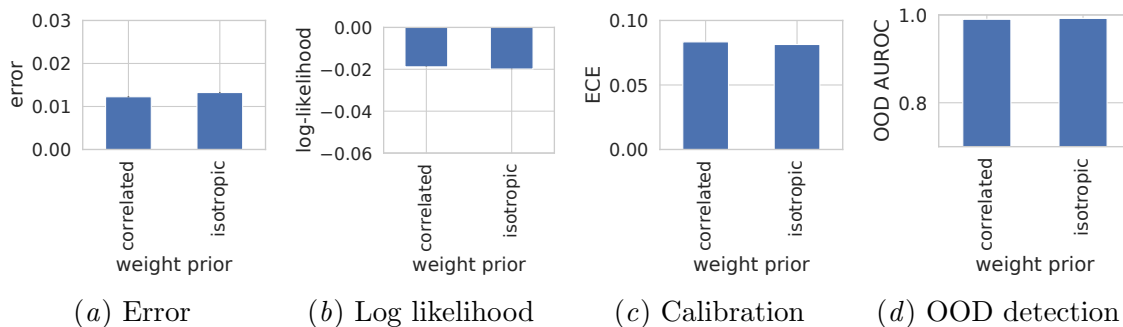(a) Error   (b) Log likelihood   (c) Calibration   (d) OOD detection

Figure B.11: Performance of Bayesian CNNs with different priors on MNIST in terms of different metrics. We see that the correlated prior performs a bit better than the isotropic one.
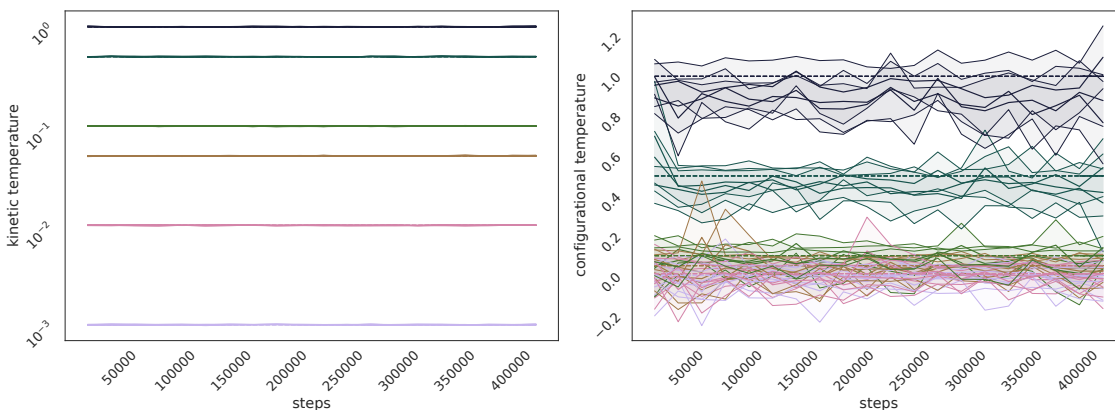

Figure C.1: Temperature diagnostics of the MNIST experiment with FCNNs. The kinetic temperature estimates coincide with the desired temperature. The configurational temperature estimates are within error bars for all temperatures, but the mean is usually low. This is mild evidence that the sampler may not be entirely accurate.

where $d(\cdot, \cdot)$ is the Euclidean distance in pixel space and we set $\sigma = \lambda = 1$.

Appendix E. Evaluation Metrics

When using BNNs, practitioners might care about different outcomes. In some applications, the predictive accuracy might be the only metric of interest, while in other applications calibrated uncertainty estimates could be crucial. We therefore use a range of different metrics in our experiments in order to highlight the respective strengths and weaknesses of different priors. Moreover, we compare the priors to the empirical weight distributions of conventionally trained networks.
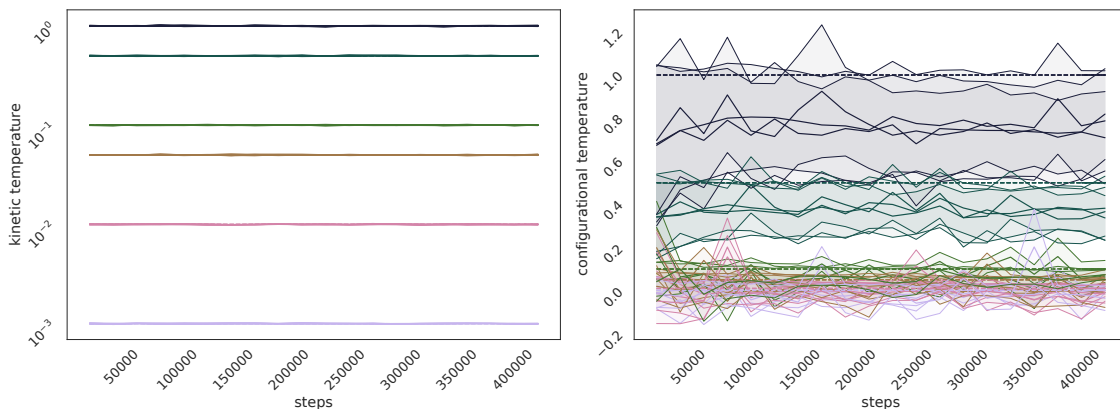
Figure C.2: Temperature diagnostics of the MNIST experiment with CNNs and heavy-tailed priors. The conclusions are similar to Figure C.2.
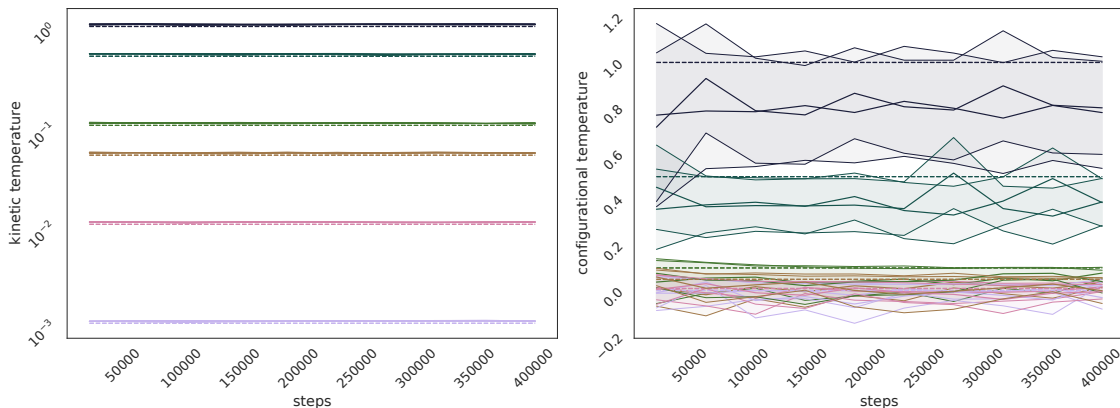

Figure C.3: Temperature diagnostics of the MNIST experiment with CNNs and correlated priors. The conclusions are similar to Figure C.2, but here the kinetic temperature is slightly too hot.

E.1. Empirical test performance

Test error   The test error is probably the most widely used metric in supervised learning. It intuitively measures the performance of the model on a held-out test set and is often seen as an empirical approximation to the true generalization error. While it is often used for model selection, it comes with the risk of overfitting to the used test set (Bishop, 2006) and in the case of BNNs also fails to account for the predictive variance of the posterior.

Test log-likelihood   The predictive log-likelihood also requires a test set for its evaluation, but it takes the predictive posterior variance into account. It can thus offer a built-in tradeoff between the mean fit and the quality of the uncertainty estimates. Moreover, it is a proper scoring rule (Gneiting and Raftery, 2007).

E.2. Uncertainty estimates

Uncertainty calibration   Bayesian methods are often chosen for their superior uncertainty estimates, so many users of BNNs will not be satisfied with only fitting the posterior mean well. The calibration measures how well the uncertainty estimates of the model correlate with predictive performance. Intuitively, when the model is for instance 70 % certain about a prediction, this prediction should be correct with 70 % probability. Many deep learning models are not well calibrated, because they are often overconfident and assign too low uncertainties to their predictions (Ovadia et al., 2019; Wenzel et al., 2020b). When the models are supposed to be used in safety-critical scenarios, it is often crucial to be able to tell when they encounter an input that they are not certain about (Kendall and Gal, 2017). For these applications, metrics such as the expected calibration error (Naeini et al., 2015) might be the most important criteria.

Out-of-distribution detection   The out-of-distribution (OOD) detection measures how well one can tell in-distribution and out-of-distribution examples apart based on the uncertainties. This is important when we believe that the model might be deployed under some degree of data set shift. In this case, the model should be able to detect these OOD examples and be able to reject them, that is, refuse to make a prediction on them.

Appendix F. Implementation details

Training setup.   For all the MNIST BNN experiments, we perform 20 cycles of SG-MCMC (Zhang et al., 2019) with 45 epochs each. We draw one sample each at the end of the respective last five epochs of each cycle. From these 100 samples, we discard the first 30 as a burn-in of the chain. Moreover, in each cycle, we only add Langevin noise in the last 15 epochs (similar to Zhang et al. (2019)). We start each cycle with a learning rate of 0.01 and decay to 0 using a cosine schedule. We use a mini-batch size of 128.

For the SGD experiments yielding the empirical weight distributions, we use the same settings, but do not add any Langevin noise. We also only take one sample at the very end of training.

FCNN architecture.   For the FCNN experiments, we used a feedforward neural network with three layers, a hidden layer width of 100, and ReLU activations.

CNN architecture.   For the CNN experiments, we use a convolutional network with two convolutional layers and one fully-connected layer. The hidden convolutional layers have 64 channels each and use 3×3 convolutions and ReLU activations. Each convolutional layer is followed by a 2×2 max-pooling layer.